Macromolecules **1987**, *20*, 1022–1029

Spectroscopic Characterization of the $\alpha \rightleftharpoons \beta$ Crystalline Phase Transition in Poly(butylene terephthalate) and Its Copolymers with Poly(tetramethylene oxide)

Eva Dobrovolny-Marand and Shaw Ling Hsu*

Department of Polymer Science and Engineering, University of Massachusetts, Amherst, Massachusetts 01003

C.-K. Shih

Du Pont Experimental Station, Wilmington, Delaware 19898. *Received October 10, 1986*

ABSTRACT: The stress-induced crystalline $\alpha \rightleftharpoons \beta$ phase transition found in poly(butylene terephthalate) and its copolymers with poly(tetramethylene oxide) has been studied by Fourier transform infrared spectroscopy coupled with mechanical measurements. The phase transformation behavior was explained in terms of a cooperative model that considered both intermolecular and intramolecular interactions within the crystal. It was shown that the strength of the intramolecular interactions increased with length of the hard segments and that the strength of the intermolecular interactions increased with perfection and lateral size of the crystals. The intermolecular interaction was assumed to be dominated by the interaction between neighboring terephthalate groups. The "mean" intramolecular energy was estimated at 0.40 kcal/mol. This calculation was based on the potential energy of rotation of a carbonyl group about a benzene–carbonyl bond. Cooperativity between chains diminished when the surface-to-volume ratio increased above 2×10^{-2} Å^{-1}.

Introduction

The mechanical response of semicrystalline polymers is dependent on the deformation mechanism available to their structures. For example, the stress hysteresis observed in the stress–strain response of poly(butylene terephthalate) (PBT) is believed to arise from two different deformation modes. One mode is the time-dependent restructuring or re-formation of the disrupted superstructure, and the other mode is the time-independent[1] stress-induced crystalline phase transition. A similar mechanism controls the deformation in the copolymers of PBT and poly(tetramethylene oxide). The reversible nature of the phase transition and its ability to absorb stress is partly responsible for the desired properties, such as resilience, dimensional stability, and toughness exhibited both by the PBT homopolymer and its copolymers. The significant factors that control the character of the transition are therefore of practical and fundamental interest.

The crystalline phase transformation in PBT has been recognized in several X-ray[2–4] and infrared[5–9] studies; however, the physical basis for its existence and the significant controlling factors still have not been clearly defined. The size of the crystalline domains, for example, or the perfection of the crystalline structure may influence the character of the transformation. This would be especially true if intra- and intermolecular interactions control the microscopic mechanism of the crystalline transition. In order to examine these variables, a means of achieving a known crystalline structure and variable crystalline size is necessary. A variable crystalline size can be obtained by utilizing the copolymer series of poly(butylene terephthalate) and poly(tetramethylene oxide). In this series, the comonomer concentration determines the average hard-segment length, which, in turn, dictates the lateral dimensions and the thickness of the crystals.[10–12] Due to the identical nature of the crystalline phase in pure PBT and that in the copolymer, the crystalline phase transition is observed in both types of polymers. The crystalline superstructure is determined by the crystallization conditions. Quenching from the melt, for example, gives rise to highly nucleated, interpenetrating lamellar morphology.[10,12,13] Coextrusion of such films at temperatures below the melting point serves to orient and anneal the crystalline domains, producing a long-range periodic superstructure.[14]

Free from tension, the PBT crystals exist in the α form which when stressed transforms into the crystalline β form. The process is reversible in that nearly all α crystals are recovered when the stress is released. Due to the difference in unit cell dimensions of the two crystalline forms, wide-angle X-ray reflections characteristic of either form have been assigned.[3,15,16] In fact, X-ray data have been used to assess the degree of transformation as a function of the applied stress.[17,18] Since the X-ray technique is only sensitive to long-range order or disorder, small isolated crystalline forms cannot be detected. Furthermore, the sample can relax substantially during the long exposure time necessary to obtain a diffraction pattern, thus perturbing the X-ray data for quantitative analysis. Simultaneous spectroscopic and mechanical measurements, on the other hand, offer an alternative technique to correlate microstructural changes with macroscopic stress–strain results directly. Infrared spectroscopy can selectively identify conformational differences such as those characteristic of the α and β crystalline forms. The high sensitivity of this technique permits the detection of isolated α or β units at all levels of applied stress.

A cooperative model can be used to explain the observed transformation behavior as a function of stress.[19] This model, which only considered attractive forces between molecular chains, could predict the change in transformation with increasing temperature. Such change consists of a decrease in the hysteresis width associated with the transformation–stress behavior. However, the model also predicted the hysteresis to disappear at a certain critical temperature, T_c. In fact, as we will show, the hysteresis persists above T_c and can be, in principle, explained by intramolecular interactions existing along the crystalline hard segment.

Our goal is therefore twofold: (1) to determine the effect of crystalline size on the transformation behavior and (2) to present a theoretical model that would consider the role of both intramolecular and intermolecular interactions in the crystalline phase transition. This is achieved by combining infrared spectroscopy with mechanical measurements to study the deformation of PBT homopolymer

0024-9297/87/2220-1022$01.50/0

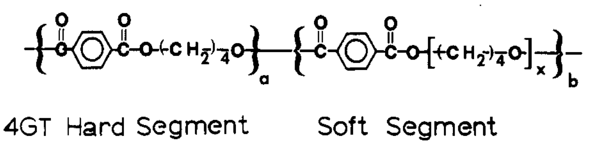

Figure 1. Molecular structure of a copolymer of poly(butylene terephthalate) with poly(tetramethylene oxide).

Table I
Summary of Experimental Samples and Corresponding Parameters

sample	x_h	L, %	x_c	T_{co}, °C	T_g, °C	T_m, °C
PBT						
P1			39.3	40	50	222
P2			39.2	80	50	222
P3			39.5	120	50	222
P4			40.2	160	50	222
copolymer						
H1	0.96	23	34.4	120	-10	216
H2	0.93	15	32.7	100	-30	211
H3	0.88	8	24.9	75	-54	200
H4	0.83	6	20.7		-60	194

films and a series of PBT copolymer films with variable hard-segment content.

Experimental Section

Sample Preparation and Characterization. Poly(butylene terephthalate), trade name Valox 310, with $\bar{M}_N$ = 20 000 was obtained from the Plastics Division of General Electric Co. The copolymers of poly(butylene terephthalate) with poly(tetramethylene oxide) were kindly supplied by Du Pont. Copolymers having a hard-segment molar fraction of 0.96, 0.93, 0.88, and 0.83 with an average molecular weight of the polyol of 1100 ($\bar{M}_n$) were used in this study. The molecular structure of the copolymers is illustrated in Figure 1.

Samples were melt-pressed between two aluminum sheets coated with Teflon and then quenched in ice water. Resulting films were oriented (draw ratio 3) by coextrusion using the split-billet technique.[20] The temperature during coextrusion was set 130 °C above the particular glass transition, T_g, of the sample. All films prepared this way were highly oriented and had a thickness of 20–50 μm. Strips of 0.5 cm × 2.5 cm were used in the deformation experiments. Percent crystallinity was determined by differential scanning calorimetry (DSC) taking H_f = 28.7 kJ/mol.[21] The hard-segment molar fraction, x_h, coextrusion temperature, T_{co}, glass transition T_g, melting temperature, T_m, calculated average hard-segment length, L, and percent crystallinity, x_c, for each sample are summarized in Table I.

Wide-angle X-ray diffraction patterns were obtained on a Statton camera with nickel-filtered Cu Kα radiation. Film thickness of 1 mm was achieved by stacking several films oriented in the same direction.

Spectroscopic and Mechanical Measurements. Simultaneous infrared spectra and stress–strain measurements were obtained on a Nicolet 7199 Fourier transform infrared spectrometer employing a Nicolet Model 7000 optical bench. A hydraulic stretcher was used to deform the sample film at a programmable stress or strain. The details of the equipment and their operations are described elsewhere.[1,22,23] Deformation experiments were carried out at 1.5% strain/min to a maximum strain of 30%, over two complete loading cycles. All spectra were collected at 4-cm^{-1} resolution.

Results and Discussion

Band Assignment. The infrared spectra are well established for PBT.[4-8] The α and β crystalline phases differ in the conformation of the central tetramethylene group. The methylene rocking region (1000–900 cm^{-1}) and the methylene bending region (1495–1440 cm^{-1}) contain infrared bands associated with the vibrational modes observed only for the α or β conformations. The methylene rocking region, Figure 2, is particularly sensitive due to its coupling with skeletal vibrations. An infrared band found at 917 cm^{-1} is characteristic of the GTG′ conformation of the tetramethylene group present only in the PBT crystalline regions, as this absorbance band is absent from the spectrum of the melt.[8] A 960-cm^{-1} band is known to have contributions from the TTT conformation of the tetramethylene group found in the crystalline and amorphous regions of the PBT hard segment. The 917- and 960-cm^{-1} bands arise primarily from a torsional mode about the C–O–C–C bond in either conformation. Another absorption is found at 935–938 cm^{-1} that has been associated with the CH$_2$ rocking vibration of the amorphous hard segments.[6] In our study the quantitative measurements of the relative changes in the α and β contents were obtained by subtracting the first spectrum of the undeformed film from all the consecutive spectra obtained during the deformation. Figure 3 shows the resulting difference for one case of PBT at 15% strain. The areas above the base line represent the increase of the β phase, $\Delta\beta$, and below the line, amount of α phase decrease, $\Delta\alpha$. These integral areas are plotted against each other in Figure 4. The plot of $\Delta\alpha$ and $\Delta\beta$ shows a linear relationship, indicating that there is an equivalent conversion of one crystalline form into the other, with no possibility left for a third component. Stress-induced crystallization can therefore be ruled out. The same conclusion has been reached by other in-

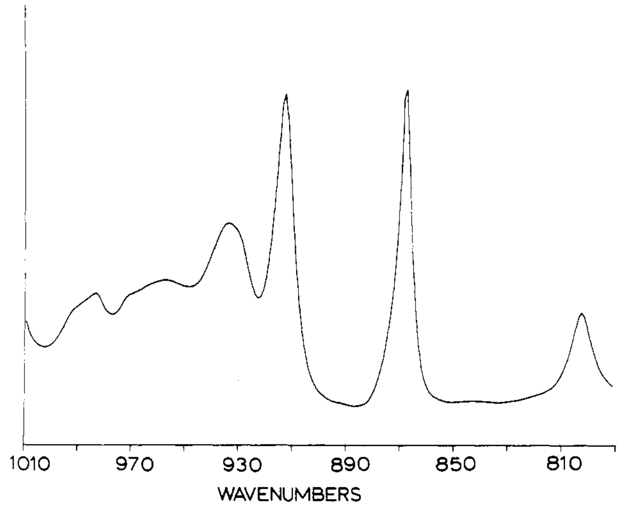

Figure 2. Methylene rocking region of poly(butylene terephthalate).

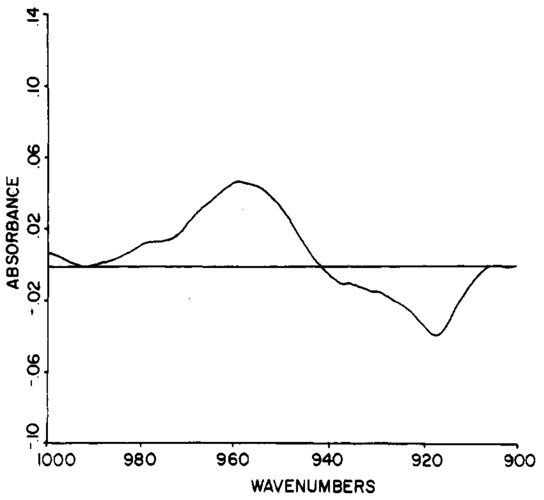

Figure 3. Spectrum obtained by subtracting the spectrum of an undeformed film from a spectrum of a deformed film strained to 15%.

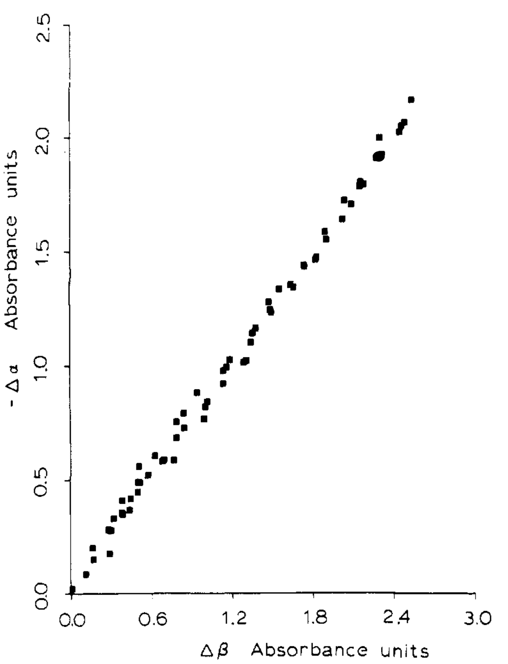

Figure 4. α and β content as determined by characteristic integrated spectral changes plotted against each other for a series of data points in two consecutive cycles.

vestigators based on factor analysis of spectra collected during several deformation cycles.[9] In the copolymer, the uncrystallized hard segments are rejected to the crystal fold surface and the surrounding matrix.[10] They seem not to participate in the transformation process, since this amorphous band (935–938 cm^{-1}) cancels during the subtraction of the spectra.

Before subtraction, all spectral intensities have been scaled to the same thickness using an internal reference band. We have used the integrated structural absorbance of the C–H stretching region as an internal standard. In order to facilitate comparison of α and β stress-induced changes between samples with different percent crystallinity, all $\Delta\alpha$ and $\Delta\beta$ values were reduced. This was accomplished by dividing by the highest expected change in α or β, i.e., $\Delta\alpha_{max}$ or $\Delta\beta_{max}$. The value of $\Delta\alpha_{max}$ was obtained by integrating the resolved 917-cm^{-1} band in the original undeformed spectrum. The value of $\Delta\beta_{max}$ was then extrapolated from the curve in Figure 4. For clarity, the relative changes of α and β contents have been represented by the change in the β content only, as one is the negative of the other, i.e., $x_\beta + x_\alpha = x_c$ and $\Delta\alpha = -\Delta\beta$.

The hard-segment orientation has been analyzed by measuring the dichroism of the C=O stretching (1716-cm^{-1}) vibration and the amorphous orientation was estimated by measuring the dichroism of the C–H stretching (2940-cm^{-1}) vibration. The transition moment directions were assumed to be 90° and 79° for the C–H and C=O stretching vibrations, respectively.[24] Because the C–H and C=O functional groups are present in both crystalline and amorphous regions their relative concentrations in both environments have to be taken into account. Therefore, the segmental orientation function, assuming a uniaxial deformation, can be calculated only if the molar fraction of the hard segments and the percent crystallinity are known and the measured dichroic values need to be weighted accordingly. We have only estimated the orientation behavior of the copolymer sample (H2). From the chemical structure and the degree of crystallinity measured, the percent of CH_2 groups in the amorphous phase was calculated to be 85% with 53% of the CH_2 groups in the soft segments themselves. Similarly, the percent of C=O groups in the hard segments was calculated to be 93% with 30% of the C=O groups being actually in the crystalline phase.

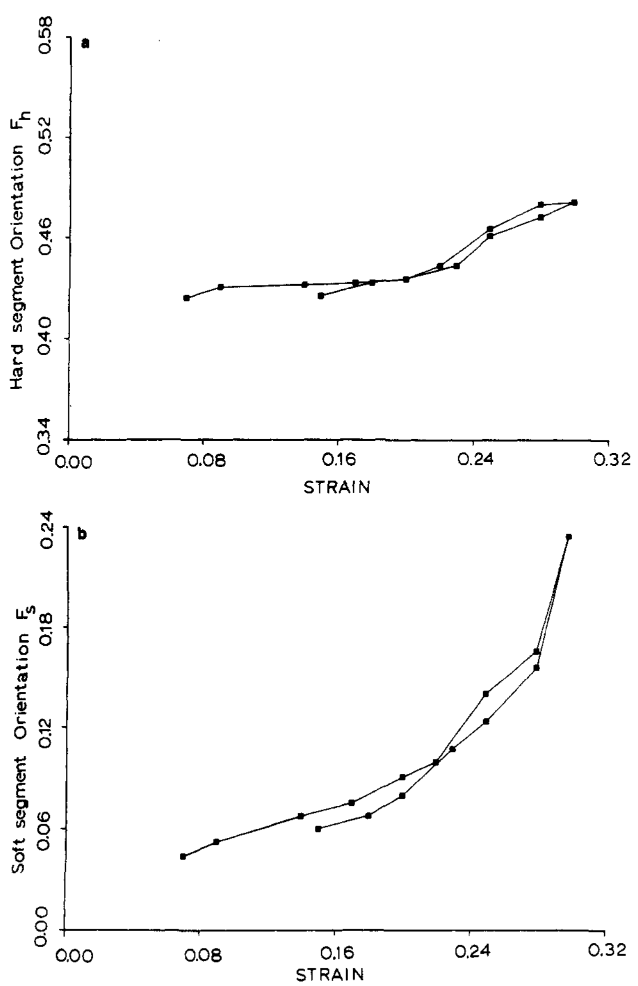

Figure 5. Orientation function as a function of strain calculated: (a) the hard segment; (b) the soft segment.

The orientation functions of the hard and soft phases are shown in Figure 5. Our data suggests that the hard segments do not orient further beyond a 30% strain value. The amorphous chains as shown in Figure 5, however, do improve their orientation continuously with increasing strain. In addition, we observed that neither component shows hysteresis in segmental orientation as a function of strain within detectable limits. These results are important, as will be seen later in that segmental orientation changes cannot account for the spectroscopic changes observed at high strain values, and only the phase transformation needs to be considered.

Crystalline Phase Transition. A typical response of the crystalline conversion over two deformation cycles is shown in Figure 6. This phase transition is not completely recoverable in the first cycle since some residual β crystals are present even at zero stress. However, the following cycles repeat the pattern outlined by the unloading and reloading curves. It is important, therefore, to separate the hysteresis caused by the plastic deformation of the crystalline superstructure from the hysteresis due to the $\alpha \rightleftharpoons \beta$ crystalline transition. Since a greater part of the plastic deformation takes place during the initial extension,[25] all hysteresis measurements will be limited to the maximum width between the subsequent unloading and reloading curves. The β fraction as a function of the applied stress for a series of molar concentrations of the hard segment (x_h) in the copolymer is shown in Figure 7.

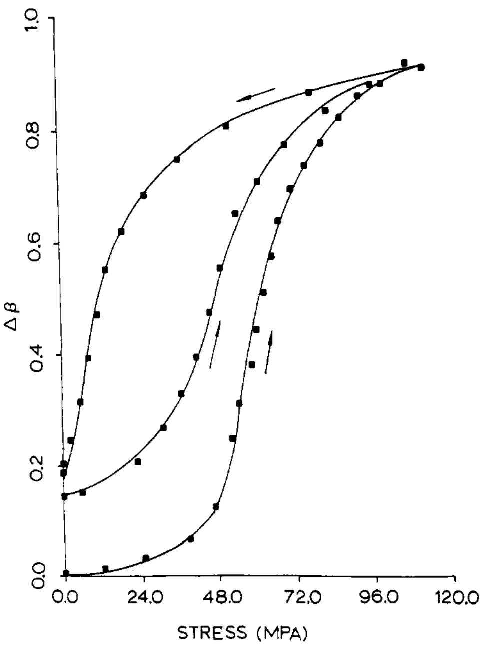

Figure 6. Change in β fraction in PBT as a function of stress over two deformation cycles conducted at room temperature.

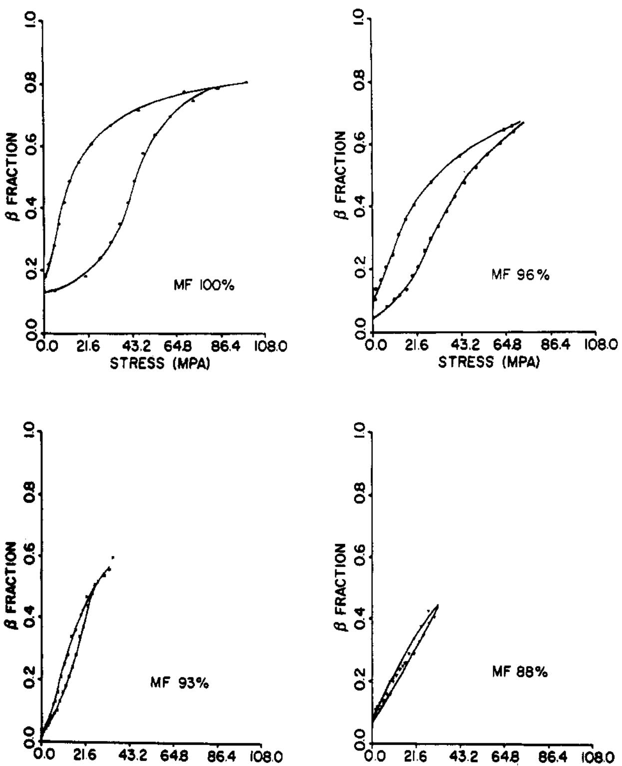

Figure 7. β fraction as a function of stress during the second loading cycle. The series of molar concentrations of the PBT hard segment x_h: (a) x_h = 100%, (b) x_h = 96%, (c) x_h = 93%, and (d) x_h = 88%, have been examined.

Comparison of β fractions during initial deformation conditions indicates that the rate of crystalline transformation with stress is slower as the average crystallizable hard-segment length increases. This suggests that α crystallites with greater dimensions are initially more restricted to transform into the β form and do so only at higher stress values. However, once this tranformation does begin, the rate of transformation becomes faster for larger crystals. Furthermore, the hysteresis between the unloading and the reloading curves decreases with decreasing x_h, being nearly zero when x_h = 88%.

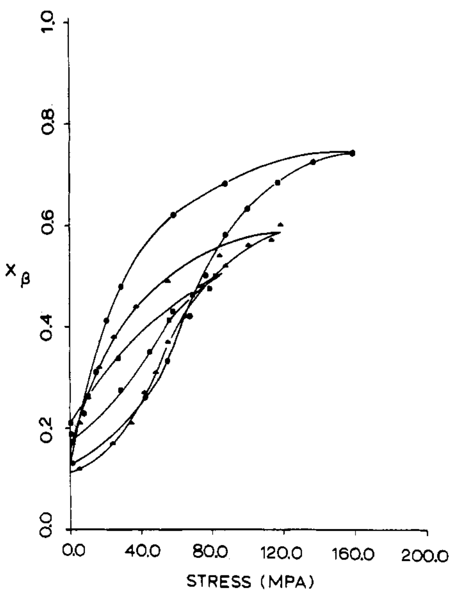

Figure 8. Hysteresis cycles observed for the phase transformation for PBT films coextruded at several temperatures: (■) 40 °C, (▲) 80 °C, and (●) 160 °C.

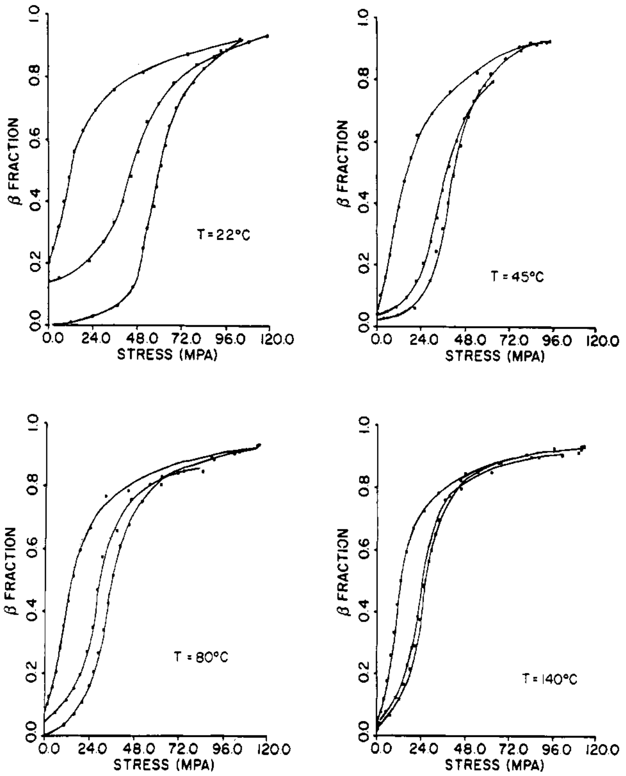

Figure 9. β fraction as a function of stress during two consecutive loading cycles of PBT film, for a series of temperatures: (a) T = 22 °C, (b) T = 45 °C, (c) T = 80 °C, (d) T = 140 °C.

This decrease in hysteresis width is also found in series of PBT samples coextruded at increasingly lower temperatures, as shown in Figure 8. The X-ray diffraction patterns corresponding to these films indicate a variation in the perfection of the crystalline structure. Samples coextruded at 160 °C have a well-defined crystal structure, whereas those subjected to the same process at a lower temperature, 40 °C, possess some crystalline disorder and defects as indicated by the presence of several diffuse reflections and complete absence of other higher order reflections observed.

The width of the hysteresis cycle is also quite sensitive to temperature as shown in Figure 9. The characteristic values of the hysteresis loop widths [32 MPA (295 K), 21 MPA (320 K), 14 MPA (335 K)] are in good agreement with similar data obtained by Brereton[17] from wide-angle X-ray diffraction [37 MPA (300 K), 24 MPA (330 K)]. However at higher temperatures, although the trend is similar, some discrepancy between the spectroscopic and X-ray results is evident. Infrared measurements indicate a slower decrease of hysteresis values with temperature [11.5 MPA (353 K), 10 MPA (415 K)] than do corresponding X-ray results [9 MPA (373 K), 3 MPA (427 K)]. The larger hysteresis values obtained from infrared measurements become especially apparent when one realizes that they have been measured between the unloading and reloading curves, whereas the X-ray hysteresis values have been measured between the first loading and unloading curves. Because of the shorter measurement time needed, we obtained a much more complete set of data with our spectroscopic studies than the earlier X-ray results. Therefore we have a greater confidence in the present study.

Theoretical Development. Theoretically, the sigmoidal behavior of the β content fraction as a function of the applied force and the decrease of hysteresis with temperature can be predicted by applying the mean-field approximation to a system of units with internal interactions that propagate order from one unit to another. This mean-field assumption was made by Datye and Taylor in their model, which assumes significant intermolecular interactions to occur only between the terephthalate residues belonging to neighboring chains.[19] These van der Waals interactions constraining the aromatic rings to remain in registry are modeled as Hookean springs. Thus dimensional changes in the lattice prompted by the crystalline transition will be hindered, especially when the transformation occurs from species present in large concentrations to those present in very low concentrations. However, as presented, Taylor's model does not take into consideration the influence of crystallite size, which our experimental results show to be significant. In particular, the effect of the hard-segment length needs to be incorporated into the model, because the intramolecular interactions along the crystalline chain should be of considerable importance. These arise from the different placement of the terephthalate residues in the α and β crystalline unit cells. In the α form, the plane of the benzene rings is inclined approximately 19° to the c axis of the unit cell, whereas in the β form, the plane of the benzene rings is nearly parallel to the c axis. When unlike tetramethylene conformations share the same benzene ring, their energies will be perturbed owing to the ill-defined chain packing. A schematic representation of this concept is depicted in Figure 10, where a unit having an all-trans conformation of the tetramethylene connects to terephthalate groups having two different inclinations of the benzene planes.

Considering only the repeat units along one chain, one can write the conformational energy of a chain, n units long, as the sum of the energies of the separate units and the energy of interaction between these units, ΔE

$$E(\text{chain}) = \sum_{k=1}^{n} E(k) + \Delta E(1, 2, ..., n) \qquad (1)$$

where

$$\Delta E\ (1, 2, ..., n) = \tfrac{1}{2}! \sum_{a \neq b}^{n} \sum_{b=1}^{n} E(a,b) \qquad (2)$$

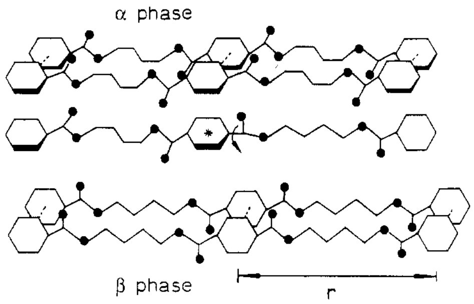

Figure 10. Schematic representation of a crystalline chain where two tetramethylene segments in α and β conformations share the same terephthalate group (designated by an asterisk). The unlike planarity of the aromatic ring required by the two conformations is responsible for the higher potential energy of the crystalline chain.

This term is incorporated into the Hamiltonian for the total system having N as the total number of units in the lattice, where m is the number of chains in a cross-sectional area and n is the number of units in the chain defining the crystal thickness. The value K is the interchain interaction force constant, and F is the force along the chains. One obtains

$$H = -Kb^2 \sum_{ijk}^{N} [(\sigma_{ijk}\sigma_{i+1,jk}) + (\sigma_{ijk}\sigma_{i,j+1,k})] + \sum_{ijk}^{N} e \sum \sigma_{ijk} + \sum_{ij}^{m} \tfrac{1}{2}q \sum_{a=1}^{n} \sum_{b=1}^{n} 1 - \frac{(\sigma_{ka} + \sigma_{kb})}{2} - Fb \sum_{ijk}^{N} \sigma_{ijk} + \text{constant} \qquad (3)$$

where $b = {}^1/_2\,(r_\beta - r_\alpha)$, the r_β or r_α being the lengths of the tetramethylene in either of the two conformations with corresponding energies E_α and E_β and $e = {}^1/_2(E_\beta - E_\alpha)$. Furthermore, $E(k_a,k_b) = q$ if $r_{ka} \neq r_{kb}$ and 0 if $r_{ka} = r_{kb}$. Here q is the intramolecular interaction energy per repeat unit. The value σ_{ijk} will be 1 or −1 according to whether the repeat unit at position ijk assumes a β or an α conformation, respectively. The absolute sign in the third term is necessary because the energy of the chain is the lowest at either conversion extreme, i.e., all α or all β units. With a mean-field approximation, the Hamiltonian becomes

$$H_{\text{MF}} = -2NKb^2\langle\sigma\rangle^2 + Ne\langle\sigma\rangle - \frac{N(n-1)^2}{(n+1)n^2}Q|\langle\sigma\rangle| - NbF\langle\sigma\rangle + \text{constant} \qquad (4)$$

where Q is the mean value of q. The entropy of the system is given by

$$S = -Nk_{\text{B}}[p \ln p + (1-p) \ln (1-p)] \qquad (5)$$

where $p = (\langle\sigma\rangle + 1)/2$. Minimization of the free energy ($H_{\text{MF}} - TS$) with respect to p and rearranging yield an explicit solution for the applied force

for $\langle\sigma\rangle > 0$

$$F = 1/b[k_{\text{B}}T \operatorname{arctanh}(\langle\sigma\rangle) - 4Kb^2\langle\sigma\rangle] + e/b - \frac{(n-1)^2}{n(n+1)}\frac{Q}{2}\frac{1}{b} \qquad (6)$$

for $\langle\sigma\rangle < 0$

$$F = 1/b[k_{\text{B}}T \operatorname{arctanh}(\langle\sigma\rangle) - 4Kb^2\langle\sigma\rangle] + e/b + \frac{(n-1)^2}{n(n+1)}\frac{Q}{2}\frac{1}{b} \qquad (7)$$

The width of the hysteresis therefore varies as

$$\Delta F = 1/b\left[8Kb^2\langle\sigma\rangle - 2k_{\text{B}}T \operatorname{arctanh}(\langle\sigma\rangle) + \frac{(n-1)^2}{(n+1)n}Q\right] \qquad (8)$$

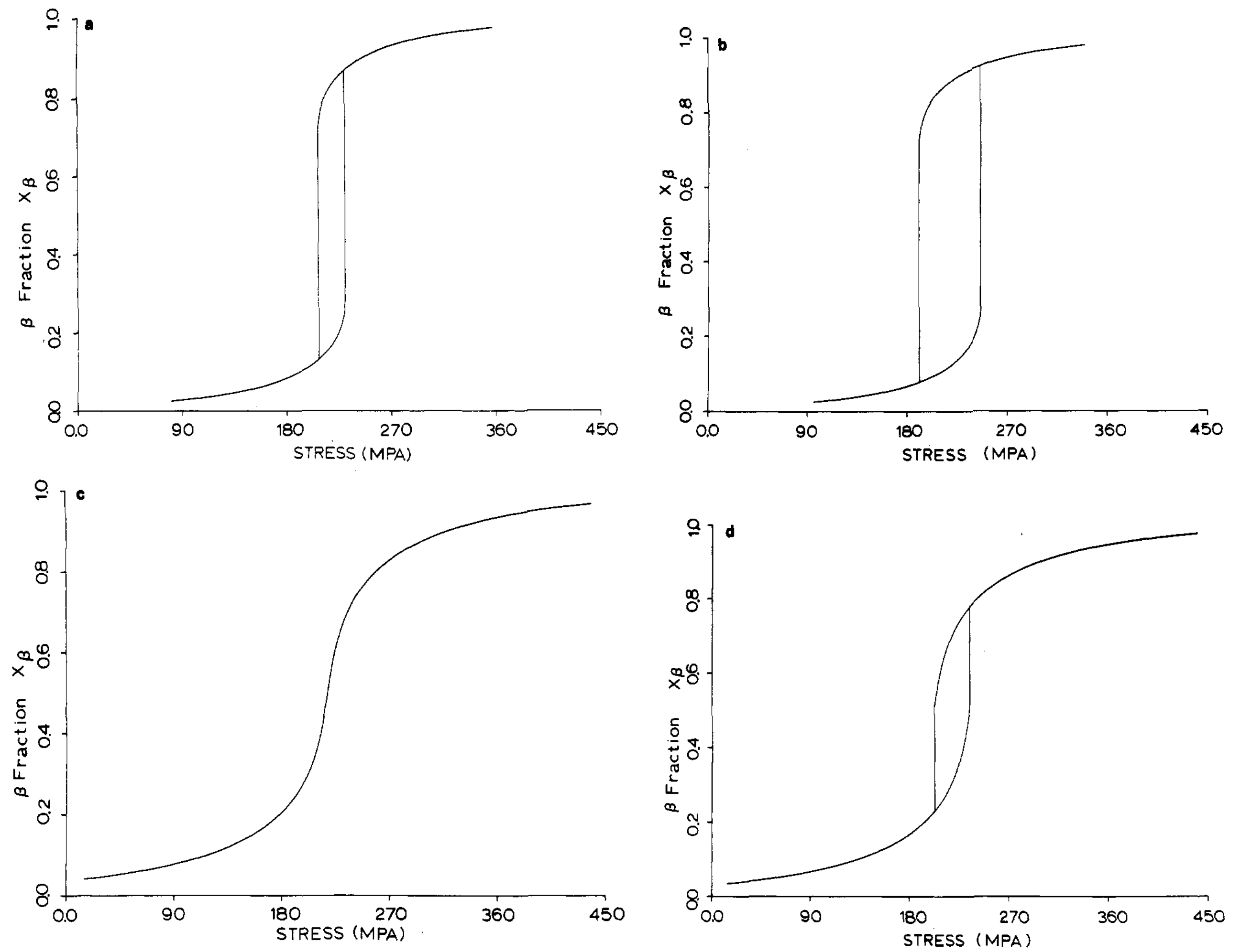

Figure 11. β fraction as a function of stress as predicted by the modified mean-field theory: (a) $T = 300$ K, $Q = 0$ kcal/mol; (b) $T = 300$ K, $Q = 0.4$ kcal/mol; (c) $T = 400$ K, $Q = 0$ kcal/mol; (d) $T = 400$ K, $Q = 0.4$ kcal/mol.

Figure 11 shows the effect that temperature and the incorporation of Q have on the width of the hysteresis, ΔF. As is evident from the equations, the sensitivity of ΔF to Q will increase as the crystallizable chain length, n, increases. In addition, as long as Q has a finite value, hysteresis will be present regardless of the temperature.

On the basis of the orientational behavior examined in our study, a quantitative analysis requires two important assumptions. They are (1) since the hard-segment orientation stays nearly constant throughout the 30% strain, the sigmoidal shape of the transformation curves cannot arise from the stress or strain-dependent orientation of the crystalline domains and (2) the hysteresis cycle observed in the $\alpha \rightleftharpoons \beta$ transition does not result from any type of hard-segment orientation relaxation. These two assumptions are valid based on the data shown in Figure 5.

Our spectroscopic data suggest that the phase transition depends on the crystalline dimensions. As the average hard-segment length decreases, the transformation of β fraction with stress becomes less sigmoidal in shape and the width of the stress hysteresis also decreases. Such behavior implies a decrease in cooperative strength. The cooperativity between the hard segments originates from the interchain retractive forces that hold the lattice together. Cooperativity along the hard segments arises from trying to prevent intramolecular interactions that occur between units with unlike conformations. The coherence is greater for larger crystals in both types of interactions. Once these barriers are overcome, the transformation becomes increasingly easier up to the near depletion of the α form. Theoretical predictions are in agreement with this picture. According to the mean-field model proposed, the hysteresis width should be partly determined by the value of Q, the average intramolecular interaction, whose relative contribution is controlled by n, the crystalline chain length, and K, whose value reflects the strength of the intermolecular interactions.

If Q equaled zero, the change of $(\Delta F)^{2/3}$ with temperature should yield a linear line according to

$$(\Delta F)^{2/3} = \left(\frac{16Kb}{3}\right)^{2/3}(1 - T/T_c) \qquad (9)$$

This clearly is not the case due to the presence of an offset in ΔF that prevents ΔF from reaching zero at $T_c = 415$ K as originally predicted.[19] This is shown in Figure 12. According to the modified mean-field theory, this offset should arise from the contribution of $(n - 1)Q/n(n + 1)$.

Although the exact relationship between the average hard segment length, L, and the corresponding crystal thickness, n, is not known, the value of n can, nevertheless, be estimated as follows. Lamellae thickness was observed on the order of 75–100 Å for the PBT copolymer having a 0.79 mol fraction hard segment.[26] Since the length of the repeat unit is approximately 12 Å, it seems reasonable to assume that there are between 6 and 8 units in this copolymer. Also, its melting point is at 186 °C. The higher melting temperature of the samples we have used suggests that their lamellar thicknesses must be greater than 75–100 Å. Using the relationship $T_m = T_m^0 - c/L$[27] with $T_m^0 = 509$ K,[21] we estimate the number of units defining the homopolymer crystal thickness between 22 and 29. On the

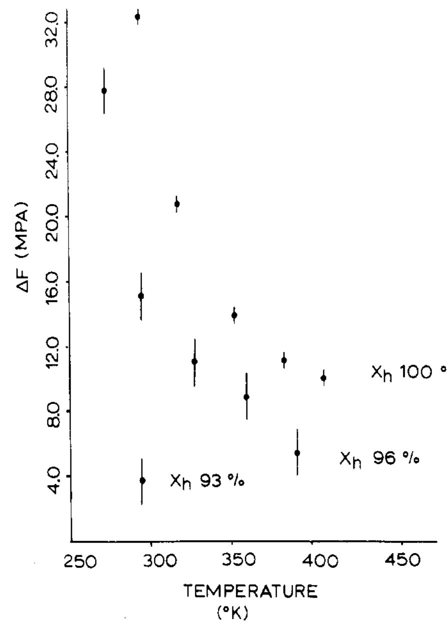

Figure 12. Hysteresis width estimated from the plots of β fraction vs. stress. The hysteresis width is plotted as a function of temperature for two mole fractions of hard segment, x_h = 100% and x_h = 96% and at one temperature for x = 93% mole fraction of hard segment.

Table II
Calculated Number of Repeat Units Defining the Crystal Thickness *n*

sample	*n*	sample	*n*
PBT	22–29	H3	8–11
H1	15–20	H4	7–9
H2	12–16		

basis of the melting points of the other copolymers, the number of repeat units traversing their crystals can also be estimated. These values are listed in Table II. It should be stressed that these values are only an estimation. More exact values can only be determined from diffraction methods.

We can get an idea of the magnitude of Q by considering the case where a terephthalate group is shared by a tetramethylene segment in an α and a β conformation on either side. If the benzene ring has the same placement and tilt as it would had it been in a perfect α crystal, the carbonyl group on the β conformation side has to rotate 20° about the ϕ–C bond in order to accommodate the extended tetramethylene conformation in the crystal. The resistance to this rotation can be estimated from the sum of nonbonded interactions of the ester group and an intrinsic twofold torsional potential resulting from the delocalization of π-electrons over the entire terephthalate residue. Rotational barrier of 0.4 kcal/mol (1.67 kJ/mol) was estimated from a potential energy–rotational angle plot.[28]

Since the width of the stress hysteresis, ΔF, for pure PBT at 293 K is 32 MPA or 1.7 kcal/mol, (multiplying by the cross-sectional area of the unit cell and the length of the repeat unit), the contribution of the calculated intramolecular potential to this value is significant. The offset measured in the hysteresis of the PBT homopolymer is equivalent to 0.30 $\mp$ 0.05 kcal/mol. Since this offset is just $Q(n-1)/(n+1)n$, then considering a chain length of 22–29 repeat units, this value must equal between 0.35 and 0.36 kcal/mol. The measured offset for the H1 copolymer is 0.20 $\mp$ 0.05 kcal/mol. With the assumption that n is between 15 and 20 repeat units, the calculated offset should be 0.32 to 0.34 kcal/mol.

However, subtraction of these estimated offset values from the measured ΔF values and calculation of $(\Delta F)^{2/3}$ still does not lend a linear line. This means that the intramolecular interactions must also decrease with temperature. Hence, one would expect the stress hysteresis to drop to zero near the melting point, where the structural coherence is lost. Unfortunately, due to the softening of the films and inability to generate sufficient stress for complete transformation, deformation experiments at temperatures higher than 160 °C are difficult.

The values of r_α, r_β, E_α, and E_β have been obtained from literature[3] and are 1.16 nm, 1.30 nm, −6.60 kJ/mol, and −1.21 kJ/mol, respectively. Since the force constant K represents the strength of cohesion between terephthalate groups in the crystalline matrix, disruption of order in the crystalline lattice by the introduction of defects or partial separation of lateral faces by shearing will decrease the value of K. The fact that the width of the hysteresis, as measured from the infrared data, decreases with decreasing perfection of the crystal structure seems to support this concept. However, there may be another possible explanation for this observation. As already mentioned, the crystalline size affects the coherence of the intermolecular interactions. When the crystallites become too small, the mean-field approximation may not be valid, because the interactions are no longer uniform. Interactions at the crystalline–amorphous interface, for example, may perturb the crystalline retractive forces, when the surface-to-volume ratio of the crystallite becomes too large. This may indeed be the situation in the samples with lower perfection of the crystal structure as well as in those with lower hard segment content, where the crystals are small. In fact, a morphological study using electron microscopy has shown that the lateral dimensions of the single-crystal lamellae vary between 10 μm × 25 μm to less than 5 μm × 10 μm from 93% to 83% mole fraction hard segment.[12] With the lamellar thicknesses estimated previously (Table II), the surface-to-volume ratios for the two samples have been derived. These are 1.2×10^{-2} and 2.1×10^{-2} Å^{-1} for 93% to 83% mole fraction hard segment. Since the hysteresis practically vanishes in samples having less than 93% mol fraction hard segment, cooperativity between chains must diminish when the surface-to-volume ratio of the crystals increases above 1.2×10^{-2} Å^{-1}.

The value of K was estimated from the hysteresis width obtained by subtracting the estimated offset value from the measured hysteresis width at room temperature. So calculated values are 153 and 147 kJ/mol nm^2 for the PBT homopolymer and the copolymer with 0.96% mol fraction hard segment, respectively. For copolymers with 0.93 and 0.88 mol fractions, $K < 140$ kJ/mol nm^2. The decrease in the K constant reflects the higher concentration of lattice imperfections and greater surface-to-volume ratio of crystals present in samples with lower mole fraction hard segment.

Conclusion

Despite the simplicity of the mean-field model, we have shown that it can be used qualitatively to understand the nature of the crystalline phase transition in poly(butylene terephthalate) and its related copolymers. The retractive forces arising from both intramolecular and intermolecular interactions are primarily responsible for the observed hysteresis and sigmoidal behavior of crystal transformation with stress. The strength of the intramolecular interactions depends on the length of the hard segment that governs the thickness of the crystal lamellae, while the intermolecular interactions vary with the perfection and size of the crystallites themselves.

Acknowledgment. This research has been supported by the National Science Foundation Polymers Program, No. DMR 8640536. We are also grateful to the Du Pont Experimental Station for making the polymers available to us.

Registry No. Poly(butylene terephthalate) (SRU), 24968-12-5; poly(butylene terephthalate) (copolymer), 26062-94-2; (poly(butylene terephthalate))(poly(tetramethylene oxide)) (block copolymer), 106159-00-6.

References and Notes

(1) Lasch, J. E.; Burchell, D. J.; Masoaka, T.; Hsu, S. L. *Appl. Spectrosc.* **1984**, *38*(3), 351.
(2) Boye, C. A., Jr.; Overton, J. R. *Bull. Am. Phys. Soc., Ser. 2* **1974**, *19*, 352.
(3) Yokouchi, M.; Sakakibara, Y.; Chatani, Y.; Tadokoro, H.; Tanaka, T.; Yoda, K. *Macromolecules* **1976**, *9*(2), 266.
(4) Jakeways, R.; Ward, I. M.; Wilding, M. A.; Hall, I. H.; Desborough, I. J.; Pass, M. G. *J. Polym. Sci., Polym. Phys. Ed.* **1975**, *13*, 799.
(5) Ward, I. M.; Wilding, M. A. *Polymer* **1977**, *18*, 327.
(6) Stambaugh, B.; Lando, J. B.; Koenig, J. L. *J. Polym. Sci., Polym. Phys. Ed.* **1979**, *17*, 1063.
(7) Holland-Moritz, K.; Siesler, H. W. *Polym. Bull. (Berlin)* **1981**, *4*, 165.
(8) Gillette, P. C.; Dirlikov, S. D.; Koenig, J. L; Lando, J. B. *Polymer* **1982**, *23*, 1759.
(9) Gillette, P. C.; Lando, J. B.; Koenig, J. L. *Polymer* **1985**, *26*, 235.
(10) Cella, R. J. *J. Polym. Sci., Polym. Symp.* **1973**, *No. 42*, 727.
(11) Wegner, G.; Fujii, T.; Meyer, W.; Lieser, G. *Angew. Makromol. Chem.* **1978**, *74*(1204), 295.
(12) Briber, R. M.; Thomas, E. L. *Polymer* **1985**, *26*, 8.
(13) Stein, R. S.; Misra, A. *J. Polym. Sci., Polym. Phys. Ed.* **1980**, *18*, 327.
(14) Bandara, U.; Dröscher, M.; Thomas, E. L. *Colloid Polym. Sci.* **1984**, *262*, 538.
(15) Mencik, Z. *J. Polym. Sci., Polym. Phys. Ed.* **1975**, *13*, 2173.
(16) Desborough, I. J.; Hall, I. H. *Polymer* **1977**, *18*, 825.
(17) Brereton, M. G. Davies, G. R.; Jakeways, R.; Smith, T.; Ward, I. M. *Polymer* **1978**, *19*, 17.
(18) Alter, U.; Bonart, R. *Colloid Polym. Sci.* **1980**, *258*, 332.
(19) Datye, V. K.; Taylor, P. L. *Macromolecules* **1985**, *18*(4), 671.
(20) Zachariades, A. E.; Mead, W. T.; Porter, R. S. *In Ultrahigh Modulus Polymers*; Ciferri, A., Ward, I. M., Eds.; Applied Science: London, 1978.
(21) Hasslin, H. W.; Dröscher, M.; Wegner, G. *Makromol. Chem.* **1980**, *181*, 301.
(22) Burchell, D. J.; Lasch, J. E.; Farris, R. J.; Hsu, S. L. *Polymer* **1982**, *23*, 65.
(23) Burchell, D. J.; Lasch, J. E.; Dobrovolny, E.; Page, N.; Domian, J.; Farris, R. J.; Hsu, S. L. *Appl. Spectrosc.* **1984**, *38*, 343.
(24) Fraser, R. D. B. *J. Chem. Phys.* **1953**, *21*(9), 1511.
(25) Siesler, H. W. *J. Polym. Sci., Polym. Lett. Ed.* **1979**, *79*, 453.
(26) Zhu, L.-L.; Wegner, G. *Makromol. Chem.* **1981**, *182*, 3625.
(27) Schultz, J. M. *Polymer Materials Science*; Prentice Hall: Englewood Cliffs, N.J.; 1974.
(28) Tonelli, A. E. *J. Polym. Sci., Polym. Lett. Ed.* **1973**, *11*, 441.

Fast Atom Bombardment Mass Spectrometry Identification of Oligomers Contained in Poly(ϵ-caprolactam) and Poly(butylene isophthalate)

Alberto Ballistreri,[†] **Domenico Garozzo,**[†] **Mario Giuffrida,**[‡] **and Giorgio Montaudo***[†]

Dipartimento di Scienze Chimiche, Università di Catania, 95125 Catania, Italy, and Istituto per la Chimica e la Tecnologia dei Materiali Polimerici, Consiglio Nazionale delle Ricerche, 95125 Catania, Italy

Aldo Filippi and Cesare Guaita

Tecnopolimeri S.p.A. (SNIA Group), Ceriano Laghetto, 20100 Milano, Italy

Piero Manaresi and Francesco Pilati

Istituto Chimico, Facoltà di Ingegneria, Università di Bologna, 40100 Bologna, Italy.

Received July 11, 1986

ABSTRACT: Fast atom bombardment mass spectrometry (FAB-MS) and high-performance liquid chromatography (HPLC) were used to identify oligomers formed in polymerization reactions leading to poly(ϵ-caprolactam) and poly(butylene isophthalate). The results indicate that FAB-MS is suitable for the rapid analysis and identification of these complex mixtures, yielding better results with respect to conventional electron impact and chemical ionization–MS modes. Metastable scanning of FAB ions, employing also collision-activated decomposition (CAD), was used in order to ascertain the fragmentation pathways of some molecular ions corresponding to cyclic oligomers of poly(ϵ-caprolactam). Positive and negative FAB mass spectra, CAD B/E and CAD B^2/E scans, are reported and discussed in the text. Definite advantages of the FAB method over conventional MS are the ability to detect labile compounds (as in the case of poly(butylene isophthalate)) and reveal higher molecular weights (up to 1450 amu, in the present case).

Introduction

The production of high molecular weight polymers is often accompanied by the formation of sizable amounts of low molecular weight oligomers.[1-3]

Among the classes of polycondensates, in particular for industrial applications, polyesters and polyamides, where often cyclic and open-chain oligomers are formed during the polymerization reactions, are the most important. In this case, knowledge of the structure and of the amount of these oligomers may be essential for obtaining high-quality industrial polymers.

Current methods for detecting low amounts of oligomers contained in polymeric samples are based almost exclusively on gas–liquid and gel permeation chromatography.[1,2] These separation techniques are indeed powerful, but sometimes low volatility of samples or low solubility in most organic solvents makes alternative and rapid methods of detection and identification for low molecular weight compounds desirable.

Mass spectrometry (MS) is particularly suitable to the detection of these materials. Up to now, the MS method most used for the detection of oligomers contained in

---

[†] Università di Catania.

[‡] Consiglio Nazionale delle Ricerche.

0024-9297/87/2220-1029$01.50/0 © 1987 American Chemical Society